JOURNAL OF SOLID STATE CHEMISTRY 79, 75–85 (1989)

A Study of the Ordering of Oxygen Vacancies in the Nonstoichiometric Perovskite $Sr_2LaFe_3O_{8+y}$ by Mössbauer Spectroscopy and a Comparison with $SrFeO_{3-y}$

P. D. BATTLE, T. C. GIBB,* AND S. NIXON

Department of Inorganic and Structural Chemistry, The University, Leeds, LS2 9JT, England

Received July 13, 1988; in revised form November 15, 1988

The nonstoichiometric perovskite $Sr_2LaFe_3O_{8+y}$ ($0 < y < 0.6$) has been studied by Mössbauer spectroscopy, X-ray powder diffraction, and magnetic susceptibility techniques. Evidence was found for two new ordered vacancy phases. Orthorhombic $Sr_2LaFe_3O_8$ is an antiferromagnet ($T_N = 715 \pm 5$ K), and is believed to contain layers of iron cations in tetrahedral coordination, each separated by two layers in octahedral coordination to oxygen. Mössbauer data gave clear indications of a second phase which was less well defined, but appears to have a range of stoichiometry below the ideal composition of $Sr_2LaFe_3O_{8.5}$ and orders antiferromagnetically at about 500 K. This "tetragonal" phase shows considerable similarity to the previously reported $SrFeO_{2.75}$, and the possibility of a structural relationship is discussed.

Introduction

The perovskite $SrFeO_3$ is of unusual interest, not only because it is one of the few oxide phases to contain iron in the +4 oxidation state, but also because it can be grossly oxygen deficient. A major investigation of oxygen deficiency in this system in our laboratory (*1*) and, subsequently, elsewhere (*2–4*) has revealed the existence of the mixed-valence phases $SrFeO_{2.875}$ and $SrFeO_{2.75}$, both having an ordered arrangement of oxygen vacancies, in addition to $SrFeO_3$ and the fully reduced (Fe^{3+}) brownmillerite-phase $Sr_2Fe_2O_5$.

In the related calcium systems, it is known that an ordered intergrowth of the $LaFeO_3$ and $Ca_2Fe_2O_5$ lattices can take place to produce the new compound $Ca_2LaFe_3O_8$ (*5, 6*). Electron diffraction studies have elegantly demonstrated (*7–10*) that the high-temperature oxidized form of $Ca_2LaFe_3O_{8+y}$ contains a three-dimensional microdomain texture, with excess oxygen incorporated in the domain walls. We were able to show (*11*) that the degree of oxidation is dependent upon the rate of quenching, and that the microdomains may be a product of the quench itself, rather than an inherent part of the structure at high temperature.

A logical extension of this work was a major investigation of the system $Sr_2LaFe_3O_{8+y}$. In a recent paper (*12*) we described the structural and electronic behavior found in the composition range $0.6 < y$

* To whom correspondence should be addressed.

0022-4596/89 $3.00

< 1; at circa 200 K a first-order transition takes place from a high-temperature averaged-valence state, in which all the Fe cations are electronically equivalent, to a low-temperature antiferromagnetic mixed-valence state by the nominal charge disproportionation

$$2Fe^{4+} \rightleftharpoons Fe^{3+} + Fe^{5+}.$$

Mössbauer spectroscopic and X-ray powder diffraction data showed that an increasing oxygen vacancy concentration depresses the transition temperature by some 50 K and causes a degree of relaxational collapse in the magnetic hyperfine patterns. There is also some evidence for electron-trapping in the vicinity of oxygen vacancies in the averaged-valence state.

In this paper we consider the region $0 < y < 0.6$ and present evidence for the existence of two ordered vacancy phases with the idealized compositions $Sr_2LaFe_3O_8$ and $Sr_2LaFe_3O_{8.5}$, and we discuss their relationships with the $SrFeO_{3-y}$ system.

Experimental

Accurately weighed amounts of spectroscopic grade Fe_2O_3, $SrCO_3$, and La_2O_3 with stoichiometric ratios appropriate for $Sr_2LaFe_3O_8$ were ground together in a ball mill, pressed into a pellet, and initially fired in a platinum crucible at 1400°C for 4–7 days with two intermediate grindings before quenching onto a metal plate in air. Aliquots of this material were then annealed in air at 1200°C for 2 days before cooling to a controlled temperature, annealing for a further 2 days to reach equilibrium, and finally quenching, usually into liquid nitrogen to minimize further uncontrolled oxidation. Samples were also made by cooling slowly from 1200°C under flowing argon, and from 1000°C under high vacuum (10^{-4} Torr). Initial characterization in each case was by X-ray powder diffraction recorded with a *Philips* diffractometer using nickel-filtered Cu$K\alpha$ radiation. Chemical analyses for nominal Fe^{4+} content were carried out by digestion in a standardized solution of ammonium iron(II) sulfate in the presence of HCl and titration with cerium(IV) sulfate using ferroin as indicator.

Magnetic susceptibility measurements were made in the temperature range $78 < T < 300$ K using a Newport Instruments Gouy balance. Mössbauer data were collected in the temperature range $4.2 < T < 773$ K using a $^{57}Co/Rh$ source matrix held at room temperature; isomer shifts were determined relative to the spectrum of metallic iron.

Results

The oxygen parameter y for a series of samples quenched from between 200 and 1400°C into liquid nitrogen is shown in Table I. The values are considered accurate to within ±0.005, and reveal a smooth decrease in oxidation with rise in temperature. The value of $y = 0.107$ for a 1400°C quench into liquid nitrogen contrasted with $y = 0.336$ for a quench from the same temperature in air onto a metal plate. Oxygen uptake is clearly rapid at the higher temperatures and the consequences of this will be discussed later.

The low temperature preparations (600°C and below) gave a single cubic X-ray pattern, although with broad lines as described above. The corresponding Mössbauer spectra revealed an averaged-valence state at room temperature in which the iron cations are involved in a rapid electron transfer, although there was some evidence for electron trapping in the vicinity of the vacancies. At low temperatures a charge disproportionation and first-order transition to a magnetically ordered phase takes place. The features of this averaged-valence phase have already been reported (*12*).

At 900°C the X-ray data showed a clear distortion of the lattice which was initially

TABLE I

THE CHARACTERIZATION OF SAMPLES IN THE $Sr_2LaFe_3O_{8+y}$ PHASE ANNEALED AT DIFFERENT TEMPERATURES

T (°C)	y	X-ray	Mössbauer
200	0.937	Cubic a = 3.874	Averaged-valence
400	0.917	Cubic a = 3.875	Averaged-valence
500	0.791	Cubic a = 3.875	Averaged-valence
600	0.689	Cubic a = 3.880	Averaged-valence
700	0.554	Cubic a = 3.885	Averaged-valence + tetragonal
800	0.447	Tetragonal	Tetragonal
900	0.417	Tetragonal (a = 3.910, c = 3.867)	Tetragonal
1000	0.300	Tetragonal	Tetragonal + (orthorhombic)
1100	0.217	Cubic a = 3.900	Tetragonal + orthorhombic
1200	0.148	Cubic + (orthorhombic)	Orthorhombic + tetragonal
1300	0.145	Orthorhombic + cubic	Orthorhombic + tetragonal
1400	0.107	Orthorhombic + (cubic)	Orthorhombic + (tetragonal)
Argon (1200°C)	0.077	Orthorhombic	Orthorhombic
vacuo (1000°C)	0	Orthorhombic (a = 5.508, b = 11.884, c = 5.603)	Orthorhombic

assumed to be tetragonal. However, the lines are broad, and there is some evidence for weak superlattice lines such that a lower symmetry or a larger unit cell cannot be excluded. The distortion was much reduced in samples prepared both above and below this temperature, and the 900°C quenched sample was investigated in detail as representative of a new phase which will be referred to as the "tetragonal" phase in the discussion.

Above 1100°C there was clear evidence for the introduction of a new low-symmetry phase, although preliminary X-ray and Mössbauer analysis suggested that the products were multiphase. The low-symmetry material was isolated as a single phase by annealing in argon at 1200°C, or *in vacuo* ($<10^{-4}$ Torr) at 1000°C, for several days and then slow cooling, thus producing a reddish-brown material which was fully reduced to Fe^{3+} (y = 0). The X-ray pattern of the *in vacuo* preparation was extremely sharp with few overlapping lines, and the reflections and d-spacings are listed in Table II. The cell constants for the orthorhombic cell were refined using 39 of the best resolved reflections. This orthorhombic cell corresponds to $\sqrt{2}a_0 \times 3a_0 \times \sqrt{2}a_0$, where a_0 is the cubic perovskite cell parameter, and is therefore comparable to that of $Ca_2LaFe_3O_8$.

Using the detailed Mössbauer characterization of these three phases, it then became possible to interpret all the samples quenched between 200 and 1400°C into liquid nitrogen in terms of either a single phase or a two-phase mixture. In Table I, a minority component is indicated in parentheses. The X-ray data were in full agreement bearing in mind that the "tetragonal" phase often showed an essentially cubic pattern and was thus indistinguishable from the averaged-valence phase.

Orthorhombic $Sr_2LaFe_3O_8$

The calcium compound $Ca_2LaFe_3O_8$ has already been characterised (*5, 6*). The orthorhombic cell with a = 5.464, b = 11.293, c = 5.563 Å corresponds to the

TABLE II

THE X-RAY DIFFRACTION PATTERN FOR $Sr_2LaFe_3O_8$ ANNEALED *in Vacuo* (Orthorhombic: a = 5.508, b = 11.884, c = 5.603 Å)

$d_{obs.}$	$d_{calc.}$	$h\,k\,l$	$I_{obs.}$	$d_{obs.}$	$d_{calc.}$	$h\,k\,l$	$I_{obs.}$
11.881	11.884	0 1 0	w	1.864	1.865	2 2 2	w
5.941	5.942	0 2 0	w		1.864	1 6 0	
5.070	5.068	0 1 1	vw	1.812	1.812	0 5 2	vw
4.082	4.076	0 2 1	w	1.800	1.799	2 5 0	vw
3.960	3.961	0 3 0	mw	1.781	1.782	0 2 3	vw
3.931	3.928	1 0 1	mw	1.767	1.769	1 0 3	vw
3.278	3.277	1 2 1	w		1.769	1 6 1	
3.234	3.235	0 3 1	w	1.759	1.760	2 3 2	vw
2.972	2.971	0 4 0	w	1.744	1.745	3 0 1	vw
2.799	2.801	0 0 2	s	1.698	1.698	0 7 0	vw
2.789	2.789	1 3 1	vs	1.693	1.695	1 2 3	vvw
2.754	2.754	2 0 0	s	1.689	1.689	0 3 3	vvw
2.626	2.625	0 4 1	w	1.615	1.615	1 3 3	m
2.498	2.499	2 2 0	w	1.608	1.608	2 6 0	mw
	2.497	1 0 2		1.597	1.597	3 3 1	m
2.368	2.370	1 4 1	m	1.559	1.558	1 7 1	w
2.286	2.287	0 3 2	m	1.520	1.520	1 4 3	w
2.260	2.261	2 3 0	m	1.504	1.504	3 4 1	vw
2.099	2.097	2 3 1	w	1.445	1.445	2 7 0	vw
2.040	2.038	0 4 2	vw	1.441	1.440	2 3 3	vw
2.033	2.034	1 5 1	w	1.419	1.419	1 5 3	vvw
2.020	2.020	2 4 0	w	1.407	1.406	3 5 1	vvw
1.981	1.981	0 6 0	ms	1.401	1.401	0 0 4	w
1.964	1.964	2 0 2	s	1.395	1.395	2 6 2	m
1.939	1.938	2 1 2	w	1.377	1.337	4 0 0	mw
1.914	1.912	1 4 2	vw				

slightly larger cell found in $Sr_2LaFe_3O_8$. No detailed crystal structure is available, but it is generally accepted that it is derived from the cubic perovskite by an ordered arrangement of oxygen vacancies along [101] axes to give an orthorhombic unit cell with layers of iron cations in tetrahedral coordination, each separated by two layers of iron in octahedral coordination to oxygen. It is also described as the $n = 3$ term in a general series $A_nB_nO_{3n-1}$ intermediate between ABO_3 ($n = \infty$, perovskite) and $A_2B_2O_5$ (n = 2, brownmillerite), in which different structural motifs produce coherent intergrowths in various proportions along the b direction. It is therefore possible to incorporate disorder and variable composition by coherent intergrowth.

We have carried out a more detailed Mössbauer characterization of $Sr_2LaFe_3O_8$ than is available for $Ca_2LaFe_3O_8$. Examples of spectra recorded between 4.2 and 723 K are shown in Fig. 1. At 4.2 K the spectrum comprises two six-line magnetic hyperfine patterns from the octahedral and tetrahedral sites. As with $Ca_2LaFe_3O_8$ the linewidths are broader than seen in $Sr_2Fe_2O_5$ and $Ca_2Fe_2O_5$ because of the presumed disorder of the Sr and La cations. However, there is a very diffuse reflection in the X-ray spectrum at a d-spacing of ~5.5 Å which probably arises from some degree of short-range ordering. The area of the octahedral pattern at 4.2 K is 66%, in good agreement with the anticipated 2 : 1 ratio of sites. The magnetic flux density B, isomer shift δ, and quadrupole perturbation ε for

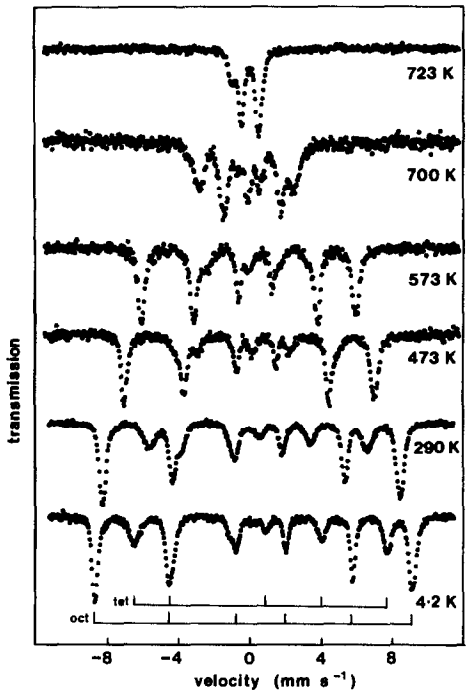

FIG. 1. Mössbauer spectra of $Sr_2LaFe_3O_8$ between 4.2 and 723 K. The octahedral and tetrahedral site patterns are shown.

TABLE III

MÖSSBAUER PARAMETERS FOR ORDERED VACANCY PHASES

Compound	T_N (K)	T (K)	B (T)	δ (mm sec^{-1})	ε (mm sec^{-1})	Site
$Sr_2Fe_2O_5$	700	295	50.1	0.37	−0.35	O
			42.2	0.17	0.30	T
		4.2	53.9	0.50	−0.36	O
			46.4	0.28	0.31	T
$Sr_2LaFe_3O_8$	715	290	52.0	0.34	−0.21	O
			38.2	0.17	0.35	T
		4.2	55.5	0.46	−0.20	O
			44.3	0.27	0.37	T
		723	—	0.06	0.93(Δ)	O
			—	−0.12	1.67(Δ)	T
$Ca_2Fe_2O_5$	725	295	51.4	0.34	−0.27	O
			43.8	0.17	0.35	T
		4.2	54.7	0.46	−0.28	O
			48.1	0.29	0.35	T
$Ca_2LaFe_3O_8$	735	290	52.1	0.36	−0.20	O
			43.0	0.19	0.29	T

each site are given in Table III, together with appropriate values from our measurements on other compounds. The magnetic flux density decreases with temperature and disappears at the Néel temperature which was determined to be 715 ± 5 K. All four compounds in Table III show very similar Néel temperatures.

The spectra at 723 K can be fitted to two symmetrical quadrupole doublets as seen in Fig. 2. The fractional intensity from the octahedral sites is now 71%, having increased slowly with temperature. This probably reflects a lower recoilless fraction at the tetrahedral site. The quadrupole perturbations ε and quadrupole splittings Δ cannot be easily correlated. Although the spin directions are almost certainly in the *ac* plane as in the brownmillerites, the probable low symmetry of the electric field gradient tensors makes detailed analysis difficult.

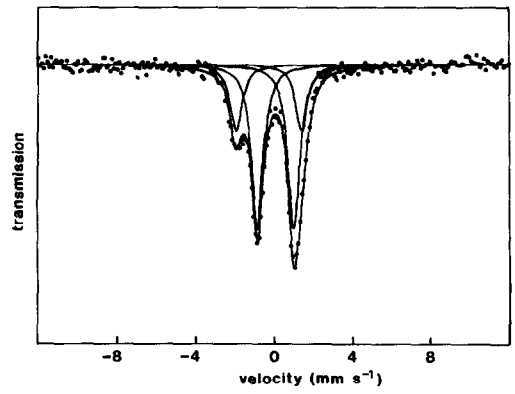

FIG. 2. The Mössbauer spectrum of $Sr_2LaFe_3O_8$ at 723 K showing the computed analysis in terms of quadrupole doublets from the tetrahedral and octahedral sites.

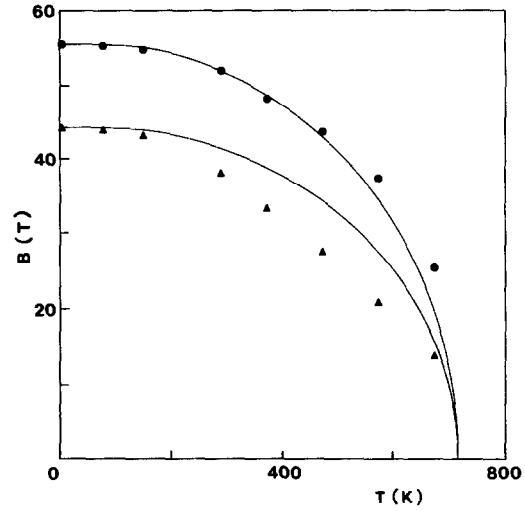

FIG. 3. The temperature dependence of the flux density of the magnetic hyperfine field, B (T), in $Sr_2LaFe_3O_8$ at octahedral (●) and tetrahedral (▲) sites. The solid curves represent the $S = 5/2$ Brillouin function.

The temperature dependence of the magnetic flux densities at the two sites are shown in Fig. 3. That for the octahedral site is reasonably close to the ideal $S = 5/2$ Brillouin function for the Fe^{3+} ion, but that for the tetrahedral site is anomalous. This behavior is not very common in Fe^{3+} ions and may reflect an anisotropy in the exchange interactions which is more extreme in $Sr_2LaFe_3O_8$ than in other related compounds. It is interesting to note that, at 290 K, the flux densities at the octahedral sites in both $Sr_2LaFe_3O_8$ and $Ca_2LaFe_3O_8$ are almost identical, whereas those at the tetrahedral sites differ by some 4.8 T. The differ-

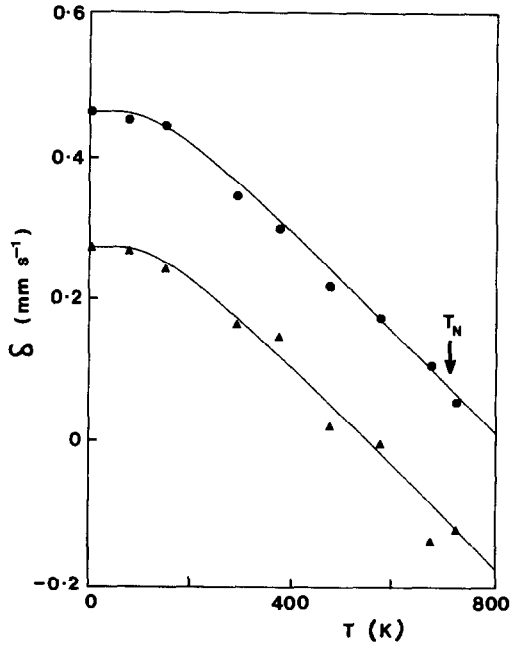

FIG. 4. The temperature dependence of the isomer shift δ for the octahedral (●) and tetrahedral (▲) sites in $Sr_2LaFe_3O_8$. The solid lines represent a simple Einstein model with θ_E = 500 K.

ence between the flux densities at the two types of site in $Sr_2LaFe_3O_8$ is also greater than that found in $Sr_2Fe_2O_5$.

The anomalously low tetrahedral site magnetic splitting results in considerable overlap of the spectral lines above 400 K, although there is no significant temperature dependence of the quadrupole perturbation parameter. The computed isomer shift values plotted in Fig. 4 show a slight scatter at higher temperatures as a result. Nevertheless, there is a good correlation between the shift values in the antiferromagnetic and paramagnetic spectra. The solid lines represent the theoretical second-order Doppler shift based on a simple Einstein model with a lattice temperature of θ_E = 500 K. The tetrahedral sites probably have a slightly lower lattice temperature, and this is in agreement with the observed decrease in the relative recoilless fractions. The spectroscopic evidence favors a high degree of ordering of the oxygen vacancies in $Sr_2LaFe_3O_8$, and we hope to carry out a full structural analysis in the near future.

"*Tetragonal*" $Sr_2LaFe_3O_{8.5}$

Typical Mössbauer spectra for $Sr_2LaFe_3O_{8.417}$ quenched into liquid nitrogen from 900°C are shown in Figs. 5 and 6. This material, which does not appear to contain significant amounts of either the cubic averaged-valence or orthorhombic phases (which show substantially different and distinct Mössbauer spectra), shows the largest "tetragonal" distortion, and is considered to be typical of the "tetragonal" phase. The 800°C quench was similar but X-ray data showed a smaller distortion. The phase can exist over the composition range $0.10 < y < 0.55$, and may be the only phase in the approximate range $0.35 < y < 0.50$. Therefore it can be considered to have a range of stoichiometry just below the ideal composition of $Sr_2LaFe_3O_{8.5}$. The material Sr_2La

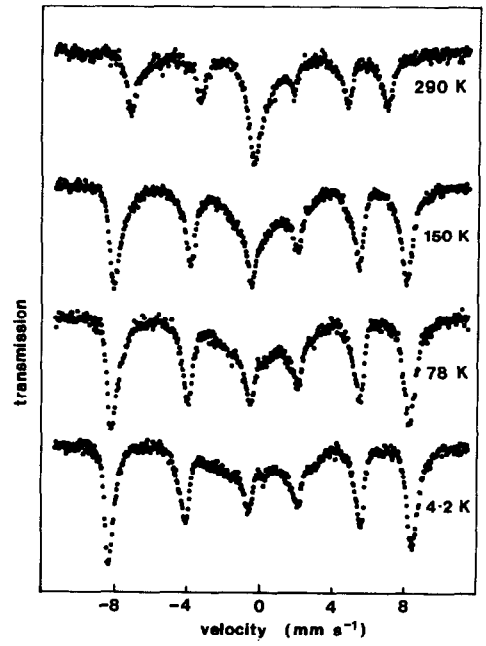

FIG. 5. Mössbauer spectra of $Sr_2LaFe_3O_{8.417}$.

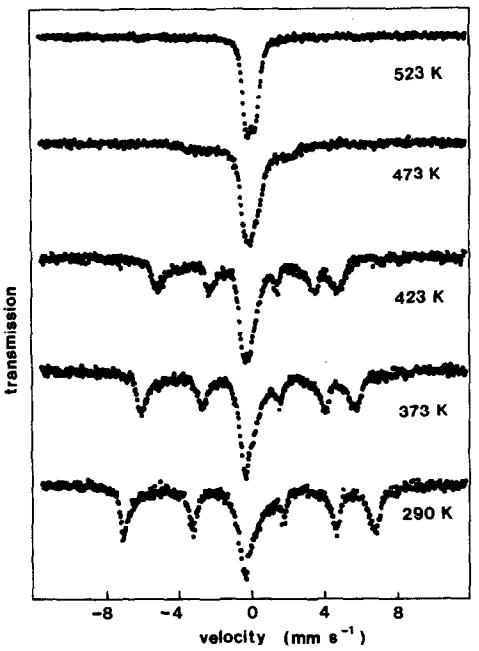

FIG. 6. Mössbauer spectra of $Sr_2LaFe_3O_{8.417}$.

$Fe_3O_{8.417}$ is magnetically ordered below 500 ± 10 K. Magnetic susceptibility data obtained between 78 and 290 K are consistent with antiferromagnetic order, but more data are required at higher temperatures before a meaningful analysis can be attempted.

The Mössbauer spectra below 423 K comprise two distinct components. First, a single magnetic hyperfine field with a saturation flux density of 51.9 T. The temperature dependence (Fig. 7) is close to the ideal $S = 5/2$ Brillouin function. The lines are somewhat broadened once again, probably due to Sr/La disorder, and comprise some 62 ± 3% of the spectrum area. The quadrupole perturbation parameter $\varepsilon = -0.32$ mm sec^{-1} at 4.2 K and appears to increase slightly with increase in temperature. The isomer shift (filled circles in Fig. 8) is typical of Fe^{3+} in octahedral coordination and shows a normal second-order Doppler shift. Second, there is a central component in the spectra which broadens gradually but without resolved structure below 290 K. The approximate isomer shift obtained by fitting a single broad Lorentzian component is shown in Fig. 8 (by the filled triangles), and is at substantially lower velocity than the averaged-valence component in the 700°C quench (*12*). The isomer shift, despite the obvious difficulties of measurement below 150 K, appears to be remarkably insensitive to temperature, and is in the range frequently found for high-spin Fe^{4+} oxides (*3*). At 473 K there is clearly a partial collapse of the magnetic component which is complete at circa 500 K. The spectrum at 523 K comprises a simple quadrupole doublet with $\delta = 0.06$ mm sec^{-1} and $\Delta = 0.46$ mm sec^{-1}. The isomer shift correlates well with the weighted average of the shift in the magnetic region. There is no reason to assign the two components to the two individual lines in the spectrum as these should not have the same intensity. Furthermore, the quadrupole interaction is not usually significantly changed by a magnetic transition, and from the equations

$$\varepsilon = \frac{e^2qQ}{8}(3\cos^2\theta - 1 + \eta \sin^2\theta \cos 2\phi)$$

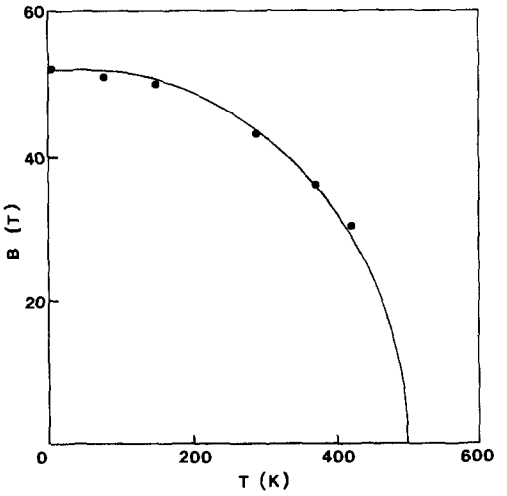

FIG. 7. The temperature dependence of the flux density of the hyperfine field, B (T), at the Fe^{3+} sites in $Sr_2LaFe_3O_{8.417}$.

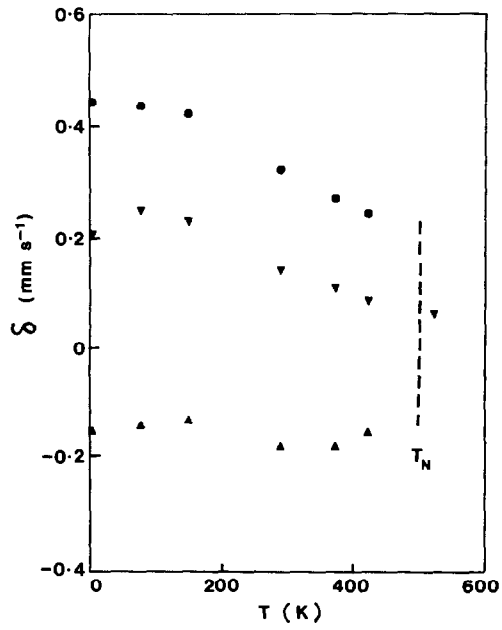

FIG. 8. The temperature dependence of the isomer shift δ for the presumed octahedral (●) and square pyramidal (▲) sites in $Sr_2LaFe_3O_{8.417}$ and their weighted average (▼).

for the quadrupole perturbation parameter in the magnetically ordered phase and

$$\Delta = (e^2qQ/2)\,(1 + \eta^2/3)^{1/2}$$

for the quadrupole splitting in the paramagnetic phase (where e^2qQ is the nuclear quadrupole coupling constant and eq, η, θ, and ϕ are the conventional parameters describing the electric field gradient tensor), it can easily be shown that $0 < |2\varepsilon/\Delta| < 1$. From the value of $\varepsilon = -0.37$ mm sec^{-1} at 423 K it follows that $\Delta \geq 0.74$ mm sec^{-1}. This is clearly not the case and the observed splitting at 523 K is thus anomalous with regard to the magnetic component. We conclude that at 523 K there is a fast electron transfer (time constant $<10^{-8}$ sec) such that all iron atoms appear electronically equivalent. The collapse in the spectrum at 473 K suggests that the electron transfer slows down and effectively ceases as magnetic order takes place and splits the electron band system. The changes are fully reversible, and there was no evidence for significant oxygen loss during the measurements.

Spectra for the quench from 800°C, $Sr_2LaFe_3O_{8.447}$, were obtained at 78, 150, and 290 K, and are basically similar to the 900°C quench, but there are some significant differences: the Fe^{3+} magnetic pattern now comprises only some 50 ± 3% of the spectrum area, and although the isomer shift of this component is unchanged, the shift of the central feature has increased from −0.17 to −0.06 mm sec^{-1}. It seems possible that this sample is actually a mixture, with a small residue of the oxygen-deficient averaged-valence phase or perhaps even an intergrowth of the two. The increase in apparent shift is certainly consistent with this interpretation.

Air-Quenched $Sr_2LaFe_3O_{8.336}$

The sample quenched from 1400°C in air, $Sr_2LaFe_3O_{8.336}$, gave an X-ray pattern which was consistent with a mixture of a poorly defined orthorhombic phase and a cubic phase. In view of the established microdomain behavior in quenched $Ca_2LaFe_3O_{8+y}$, a series of Mössbauer spectra were collected (Fig. 9). At first sight, the obvious collapse with increase in temperature which resembles a superparamagnetic behavior is consistent with a microdomain texture (*11*). However, the component which is cubic to X-rays could at least in part be the "tetragonal" phase which also shows a strong central feature at ambient temperature. A close examination of the magnetic pattern at 78 K reveals three hyperfine fields consistent with the octahedral/tetrahedral sites in $Sr_2LaFe_3O_8$ and Fe^{3+} sites in the "tetragonal" phase. However, the central feature at 290 K is far more intense than would be expected for the true "tetragonal" phase. Furthermore, it is shifted by some 0.2 mm sec^{-1} to more positive velocity. We therefore suggest that

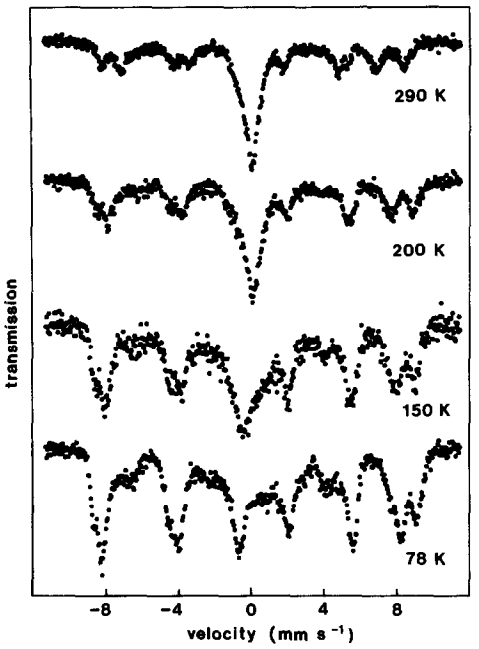

FIG. 9. The Mössbauer spectra of $Sr_2LaFe_3O_{8.336}$ quenched from 1400°C in air.

the fast quench produces a microdomain texture and intergrowth of $Sr_2LaFe_3O_8$ and the "tetragonal" phase. A more detailed examination by electron microscope should be interesting.

Discussion

In terms of integer oxidation states, $Sr_2LaFe_3O_{8.417}$ can be represented as $Sr_2La Fe^{3+}_{2.166}Fe^{4+}_{0.834}O_{8.417}$, that is, with ca. 72% of the total iron present as Fe^{3+} and ca. 28% present as Fe^{4+}. The Mössbauer spectra of this phase indicate that 62 ± 3% of the total iron is present as Fe^{3+} ions which occupy equivalent sites, probably with six- or fivefold coordination by oxygen. If we assume that all the transition metal cations take six- or fivefold coordination in exclusively corner-sharing polyhedra, then for a sample of stoichiometry $Sr_2LaFe_3O_{8.417}$, a maximum of 61% of the iron atoms can take 6-coordination. We therefore assign the magnetic sextet in the Mössbauer spectrum to 6-coordinate Fe^{3+}, and the central feature in the pattern to a mixture of the remaining Fe^{3+} and Fe^{4+}, best described as an average valence state of 3.71. An intuitive structure for the idealized composition $Sr_2LaFe_3O_{8.5}$ can be formulated on the basis of layers of Fe^{4+} in 5-coordinate sites, separated by two layers of Fe^{3+} ions in octahedral sites. This model is attractive in the sense that all the Fe^{3+} sites are potentially identical as observed experimentally. The presence of Fe^{4+} ions in square pyramidal coordination is consistent with the geometry of Mn^{3+} in the perovskite derivative $Ca_2Mn_2O_5$ ($T_N \sim$ 300 K). Layers of Mn^{3+} (high-spin $S = 2$ d^4) ions in square-pyramidal coordination occur (*13, 14*) and are illustrated in Fig. 10. It is easy to see how layers of 5-coordination could intergrow with octahedral layers. We envisage $Sr_2LaFe_3O_{8.417}$ as having a structure approximating to this ideal, but with a degree of reduction within the nominal Fe^{4+} layers, and probably some disorder in the layer sequence. The poor quality of the X-ray patterns is certainly consistent with disorder and/or a microdomain texture.

The temperature dependence of the Mössbauer signal from these predominantly Fe^{4+} layers is difficult to explain,

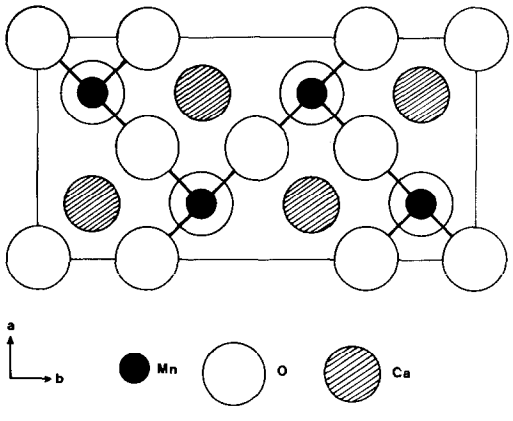

FIG. 10. An idealized illustration of the layers of square pyramidal polyhedra in $Ca_2Mn_2O_5$.

whatever the spin state we assume. Low-spin Fe^{4+} ($S = 1$) has a $^3T_{1g}$ ground state in octahedral symmetry. Under the influence of spin–orbit coupling, the ground-state becomes a singlet with $J = 0$, and hence the magnetic susceptibility falls to zero at $T = 0$ K. However the moment rapidly increases toward the spin-only value with rise in temperature. The valence contribution to the Mössbauer quadrupole splitting is sensitive to small noncubic components in the ligand field, and would be expected to be large and slightly temperature dependent. The only data available for comparison purposes (*15*) are for two diarsine complexes $[Fe(das)_2X_2]^{2-}$ (X = Cl, Br) which both showed splittings of over 3 mm sec^{-1} with no significant temperature dependence. No magnetically ordered materials are known. High-spin Fe^{4+} ($S = 2$) has an ^5E_g ground state in octahedral symmetry. There is no orbital angular momentum associated with this term, and hence spin–orbit coupling is only very weakly effective. The magnetic moment is expected to be close to the spin-only value of 4.90 Bohr magnetons. Large Jahn–Teller distortions can be expected in a localized electron system. The valence contribution to the Mössbauer quadrupole splitting will depend on the noncubic ligand field, but is very similar in principal to the more familiar Fe^{2+} in tetrahedral symmetry and should therefore be large. High-spin Fe^{4+} has been characterized in $SrLa_3LiFeO_8$ (*16*), in which the two different sites show saturation flux densities of 15.4 and 13.2 T. These are exceptionally low bearing in mind that this ground state is not expected to contribute any major orbital contribution to the field, and the argument that the contact field itself is small due to the covalency of the Fe–O bond is not very convincing. Neither high-spin nor low-spin Fe^{4+} ions with localized electrons seem fully compatible with the observed Mössbauer spectra.

The results described here represent a contribution to the study of mixed-valence, nonstoichiometric iron oxides. Specifically, they are of interest for their relevance to the much studied system $SrFeO_{3-y}$. The spectra for the "tetragonal" phase show considerable similarity to those already reported (*1–4*) for the $SrFeO_{2.75}$ phase. In that case the magnetic order takes place below ca. 220 K ($B = 45.6$ T at saturation) and is distinct from the valence-averaging above ca. 650 K. Nevertheless, the quadrupole perturbation parameter of $\varepsilon = -0.68$ mm sec^{-1} at 4.2 K has the same sign and the central component also broadens at lower temperatures but to a lesser degree. Both phases represent a similar degree of oxidation. It therefore seems plausible to seek a structural relationship between $SrFeO_{2.75}$ and $Sr_2LaFe_3O_{8.5}$ which is self-consistent.

Despite the considerable volume of data collected, the exact structure of $SrFeO_{2.75}$ remains open to argument. Both $SrFeO_{2.75}$ and $SrFeO_{2.875}$ have an ordered vacancy arrangement in a perovskite superstructure. They both undergo a transition to a cubic disordered state on heating with fast electron transfer between iron atoms (*2, 3*), and this led us to assume, erroneously, that they belonged to a single-phase material (*1*). There is some evidence to suggest that microdomains of the two phases with a coherent intergrowth can exist (*2*). It must also be remembered that all these materials are quenched from a disordered state in dynamic equilibrium, and it is therefore extremely difficult and perhaps impossible to prepare genuinely monophasic material with a lattice coherence over sufficiently large distances to give unequivocal diffraction data.

It seems to be agreed that idealized $SrFeO_{2.875}$ contains equal numbers of iron atoms as Fe^{4+} high-spin (possibly with electron delocalization as in $SrFeO_3$) and an unusual $Fe^{3.5+}$ averaged-valence state (*2–4*). Idealized $SrFeO_{2.75}$ also appears to contain equal numbers of iron atoms as Fe^{3+} (high-

spin) and Fe^{4+}. However, one school of thought favors Fe^{3+} in octahedral coordination to oxygen (on the basis of an isomer shift comparable to octahedral sites in Sr $FeO_{2.5}$) and Fe^{4+} (high-spin) stabilized in 5-coordination (*3*), whereas another proposes Fe^{3+} in 5 coordination (on the basis of a large quadrupole interaction) and Fe^{4+} in a low-spin state in octahedral coordination (*4*), and an ordered-defect model has been proposed. However, it should be noted that $Sr_2Fe_2O_5$ also shows a large quadrupole interaction at Fe^{3+} sites in 6-coordination. It is not a simple matter to resolve this controversy, because although Mössbauer data are now plentiful, it is not easy to reconcile all the observations simultaneously when some of the valence states of iron which may be involved are comparatively rare and uncharacterized. The low saturation magnetic field of 46 T for Fe^{3+} in $SrFeO_{2.75}$ was used to argue (*1*) for a low coordination despite an isomer shift more typical of 6-coordination. In retrospect we consider that the isomer shift is potentially a more reliable indicator of coordination in these materials, but even so the effect of electron delocalization, as in $SrFeO_3$, is difficult to assess. In $SrFeO_3$ the Fe^{4+} ions are nearly in a high-spin state at 4.2 K (*17*), the e_g^* and oxygen $2p$ states producing an itinerant band (there is a finite magnetic moment on the oxygen). It is tempting to suggest that alternate layers of 6 and 5-coordination can be combined to give a unit cell of $(2\sqrt{2}a_0 \times 2a_0 \times \sqrt{2}a_0)$ as observed in the X-ray data for $SrFeO_{2.75}$. However, this cell is not centered on the *ab* plane as suggested in the previously published model (*4*).

It is thus apparent that many of the ambiguities associated with the spectroscopic data collected on $Sr_2LaFe_3O_{8.417}$ are also those that have prevented a unique interpretation of the data on $SrFeO_{3-y}$.

Acknowledgments

We thank the SERC for financial support and Mr. A. Hedley for the chemical analyses.

References

1. T. C. Gibb, *J. Chem. Soc. Dalton Trans.*, 1455 (1985).
2. Y. Takeda, K. Kanno, T. Takada, O. Yamamoto, M. Takano, N. Nakayama, and Y. Bando, *J. Solid State Chem.* **63,** 237 (1986).
3. L. Fournes, Y. Potin, J. C. Grenier, G. Demazeau, and M. Pouchard, *Solid State Commun.* **62,** 239 (1987).
4. M. Takano, T. Okita, N. Nakayama, Y. Bando, Y. Takeda, O. Yamamoto, and J. B. Goodenough, *J. Solid State Chem.* **73,** 140 (1988).
5. J. C. Grenier, J. Darriet, M. Pouchard, and P. Hagenmuller, *Mater. Res. Bull.* **11,** 1219 (1976).
6. J. C. Grenier, F. Menil, M. Pouchard, and P. Hagenmuller, *Mater. Res. Bull.* **12,** 79 (1977).
7. M. A. Alario-Franco, M. J. R. Henche, M. Vallet, J. M. G. Calbet, J. C. Grenier, A. Wattiaux, and P. Hagenmuller, *J. Solid State Chem.* **46,** 23 (1983).
8. M. A. Alario-Franco, J. M. Gonzalez-Calbet, M. Vallet-Regi, and J. C. Grenier, *J. Solid State Chem.* **49,** 219 (1983).
9. J. C. Grenier, L. Fournes, M. Pouchard, P. Hagenmuller, and S. Komornicki, *Mater. Res. Bull.* **17,** 55 (1982).
10. J. M. Gonzalez-Calbet, M. Vallet-Regi, and M. A. Alario-Franco, *J. Solid State Chem.* **60,** 320 (1985).
11. T. C. Gibb, *J. Solid State Chem.* **74,** 176 (1988).
12. P. D. Battle, T. C. Gibb, and S. Nixon, *J. Solid State Chem.* **77,** 124 (1988).
13. K. R. Poeppelmeier, M. E. Leonowicz, and J. M. Longo, *J. Solid State Chem.* **44,** 89 (1982).
14. K. R. Poeppelmeier, M. E. Leonowicz, J. C. Scanlon, J. M. Longo, and W. B. Yelon, *J. Solid State Chem.* **45,** 71 (1982).
15. E. A. Paez, W. T. Oosterhuis, and D. L. Weaver, *Chem. Commun.*, 506 (1970).
16. M. F. Thomas, G. Demazeau, M. Pouchard, and P. Hagenmuller, *Solid State Commun.* **39,** 751 (1981).
17. T. Takeda, S. Komura, and H. Fujii, *J. Magn. Magn. Mater.* **31,** 797 (1983).